https://doi.org/10.15360/1813-9779-2025-3-2568



# Assessment of Structural Changes in Neutrophil Membranes Induced by Plasma from Newborns with Infection

Vladimir A. Inozemtsev[1], Igor V. Obraztsov[2], Ekaterina A. Sherstyukova[1]*, Snezhanna S. Kandrashina[1], Mikhail A. Shvedov[1], Maxim E. Dokukin[1], Viktoria A. Sergunova[1]

[1] V. A. Negovsky Research Institute of General Reanimatology, Federal Research and Clinical Center of Intensive Care Medicine and Rehabilitology, 25 Petrovka Str., Bldg. 2, 107031 Moscow, Russia
[2] G.N. Speransky Children's City Clinical Hospital No. 9, Moscow Health Department, 29 Shmitovsky pr., 123317 Moscow, Russia

**For citation:** *Vladimir A. Inozemtsev, Igor V. Obraztsov, Ekaterina A. Sherstyukova, Snezhanna S. Kandrashina, Mikhail A. Shvedov, Maxim E. Dokukin, Viktoria A. Sergunova.* Assessment of Structural Changes in Neutrophil Membranes Induced by Plasma from Newborns with Infection. *Obshchaya Reanimatologiya = General Reanimatology.* 2025; 21 (3). https://doi.org/10.15360/1813-9779-2025-3-2568 [In Russ. and Engl.]

***Correspondence to:** Ekaterina A. Sherstyukova, kmanchenko@yandex.ru

## Summary

**This study aimed** to identify neutrophil membrane characteristics that could serve as clinical biomarkers for the development of infectious complications in newborns.

**Materials and Methods.** Neutrophils isolated from healthy donors were used as a model system. The cells were incubated with plasma samples (S) isolated from blood of newborns categorized into three groups: apparently healthy (normal) (NS) ($N$=6), with localized infection (LIS) ($N$=7), and with generalized infection (GIS) ($N$=8). We assessed cellular morphology and membrane roughness before and after stimulation with phorbol 12-myristate 13-acetate (PMA) using fluorescence and atomic force microscopy. We quantified nuclear and membrane surface areas, the intensity of neutrophil extracellular trap (NET) formation, and membrane arithmetic average roughness ($R_a$).

**Results.** A standardized protocol for neutrophil preparation and evaluation was developed. Optimal incubation conditions were established; 1% bovine serum albumin (BSA) yielded minimal background activation. Dose-dependent activation of neutrophils by PMA was observed in the presence of 1% plasma. PMA stimulation significantly increased nuclear area ($P$<0.001), membrane area ($P$<0.001), and $R_a$ ($P$<0.001), regardless of plasma sample group. The most significant changes occurred in neutrophils incubated with plasma from the GIS group. Generalized infection was associated with enhanced NET activation, which may contribute to the pathogenesis of thrombotic complications in neonatal sepsis.

**Conclusion.** Microscopy-based neutrophil characteristics are promising biomarkers for evaluating infection including sepsis in newborns.

***Keywords: neutrophil membranes; newborns; infectious and septic complications; sepsis; neutrophil extracellular traps; membrane roughness; atomic force microscopy; fluorescence microscopy***

**Conflict of interest.** The authors declare no conflict of interest.

**Information about the authors:**
Vladimir A. Inozemtsev: http://orcid.org/0000-0002-4693-5624
Igor V. Obraztsov: http://orcid.org/0000-0002-6649-853X
Ekaterina A. Sherstyukova: http://orcid.org/0000-0002-9962-6315
Snezhanna S. Kandrashina: http://orcid.org/0000-0002-2185-3817
Mikhail A. Shvedov: http://orcid.org/0009-0004-4288-2758
Maxim E. Dokukin: http://orcid.org/0000-0001-6856-1953
Viktoria A. Sergunova: http://orcid.org/0000-0002-8425-0845

## Introduction

Inflammation is a universal pathological process triggered by infectious agents, mechanical or thermal injury, or major surgical interventions [1,2]. According to the epidemiological data from 2019–2020, the incidence of sepsis in the European region is approximately 750 cases per 100,000 people in developed countries [3].

Neonatal sepsis remains a major medical concern due to its high mortality rate and poor response to treatment. This is largely attributed to the immaturity of the innate immune system, which includes impaired functional activity of neutrophils and monocytes [4–6].

Studies have shown that, in cases of neonatal sepsis and multi-organ failure of mixed etiology, there is increased expression of CD64 and decreased expression of CD16 on neutrophils, which is an important diagnostic biomarker [7].

Stimulating neutrophils with physiological and pharmacological agents, such as hydrogen peroxide, lipopolysaccharides (LPS), phorbol 12-myristate 13-acetate (PMA), and calcium ionophore A23187, enhances their effector functions and induces sig-

nificant morphological changes, including transitioning from spherical to flattened shapes. This transformation is a critical component of the cell's adaptation to its protective role [8–13].

Recent studies have demonstrated that septic serum profoundly impacts neutrophils by inducing their activation and apoptosis and altering their functional properties [14, 15].

These findings underscore the importance of investigating modulatory factors that could mitigate the harmful effects of septic serum on neutrophils, with the ultimate goal of developing novel therapeutic approaches to sepsis [16].

In the present study, we performed a thorough analysis of neutrophil alterations using advanced microscopy techniques.

Despite the considerable existing research, many structural and functional aspects of neutrophils remain poorly understood. Modern optical methods are limited in their ability to elucidate neutrophil function and investigate intracellular processes [14].

In recent years, atomic force microscopy (AFM) has become increasingly utilized for investigating biological samples [17, 18], particularly cells [19–22]. AFM provides a distinct advantage by enabling the acquisition of topographic images alongside high-resolution maps of the physical properties of the cell surface [23, 24], making it a powerful tool for identifying biophysical markers.

This study aimed to identify neutrophil membrane characteristics that could serve as clinical biomarkers for the development of infectious and septic complications in neonates.

## Materials and Methods

Neutrophils were isolated from the peripheral blood of a healthy adult donor. All experimental procedures, including the collection and analysis of biological samples, were conducted in strict accordance with international ethical standards, including the 2000 Declaration of Helsinki on principles of medical research and the 1999 Council of Europe Convention on Human Rights and Biomedicine. This study was conducted in accordance with the regulatory framework and protocols of the Federal Research and Clinical Center of Intensive Care Medicine and Rehabilitology (protocol no. 427, dated October 17, 2023) and was approved by the Speransky Children's City Clinical Hospital No. 9's local ethics committee (protocol no. 45, dated May 31, 2022).

For neutrophil isolation, freshly collected donor blood was layered onto a two-step Ficoll gradient (Paneco, Russia) with densities of 1.119 g/cm³ and 1.077 g/cm³. Centrifugation was performed at 400×g for 40 minutes at room temperature. The resulting fraction containing neutrophils and residual erythrocytes was collected. The erythrocytes were lysed in ice-cold water for 30 seconds and then double-strength phosphate-buffered saline (PBS) was added to restore osmotic balance [25, 26]. The isolated neutrophils were resuspended in PBS for counting. Light microscopy confirmed that the neutrophil purity exceeded 98%, and cell viability, as assessed by trypan blue exclusion, was greater than 96%.

Experiments were conducted in 24-well plates with sterile, round coverslips in each well. To promote cell adhesion, $2\times10^5$ neutrophils were resuspended in RPMI 1640 medium (Paneco, Russia), supplemented with 10 mM HEPES (Paneco, Russia). The cells were then allowed to adhere to the coverslips for 30 minutes at 37°C in a 5% $CO_2$ atmosphere.

In all experiments, plasma samples were obtained from three groups of neonatal patients:

- NS (normal sample): apparently healthy neonates without confirmed infectious or inflammatory complications (*N*=6);
- LIS (localized infection sample): neonates with laboratory- and imaging-confirmed localized infection and no signs of organ dysfunction (*N*=7);
- GIS (generalized infection sample): neonates with a confirmed infection focus and organ dysfunction (pSOFA score>8) (*N*=8).

A total of 21 plasma samples were analyzed.

A preliminary experiment was performed to optimize the culture medium. The basal medium (RPMI 1640 + 10 mM HEPES) was compared to the same medium supplemented with 1% fetal bovine serum (FBS), 1% heat-inactivated FBS (hiFBS), or 1% bovine serum albumin (BSA) (all from Paneco, Russia). The incubation time was three hours. Based on the results, the basal medium was selected as RPMI 1640 supplemented with 10 mM HEPES and 1% BSA for subsequent experiments.

To determine the optimal plasma concentration, the basal medium was supplemented with 1%, 10%, or 50% plasma from apparently healthy neonates. The cells were then activated with 25nM PMA for three hours.

To optimize the activator concentration, 1%, 10%, or 50% normal or septic plasma was added to the basal medium. Then, the cells were activated with PMA at concentrations of 5, 10, or 25 nM for three hours.

In the main experiment, neutrophils were incubated in the basal medium supplemented with 1% plasma from each patient group. To assess activation, the cells were stimulated with 25nM PMA. The incubation period was three hours.

After the incubation period, the cells were fixed with 4% paraformaldehyde at 37°C for 30 minutes, followed by three washes with 1× PBS.

Neutrophil morphology and surface roughness were assessed using atomic force microscopy (AFM). Prior to scanning, the samples were washed three times with distilled water for 30 seconds each to remove residual salts and then dried in a Jeio Tech

VDC-11U vacuum desiccator at a pressure of $1\times10^{-3}$ MPa for one hour.

To acquire 2D and 3D images, we performed AFM scanning in semicontact mode using NTEGRA Prima and NTEGRA BIO microscopes (NT-MDT SI, Russia). NSG01 cantilevers (NT-MDT SI, Russia) with a spring constant of 5 N/m and a tip radius of 10 nm were used. Scanning was conducted at various settings: scan areas of 100×100 μm² and 2×2 μm², with 512 data points, and a scanning frequency ranging from 0.3 to 0.7 Hz.

Image analysis was performed using Gwyddion 2.65 and Image Analysis software (NT-MDT SI, Russia). The surface roughness ($R_a$) of the cells was quantified using a cutoff value of 0.440 μm to ensure maximum sensitivity and consistent analysis of all images obtained.

Widefield fluorescence microscopy was employed to evaluate neutrophil activation and measure the area of the cell membrane and nucleus. Imaging was performed using a Leica Microsystems (Germany) Thunder microscope equipped with an LED excitation source and a ×63 oil-immersion objective.

Image processing was performed using LAS X software (Leica Microsystems, Germany) and ImageJ [29]. ImageJ was used specifically for quantitative analysis of cell activation and measurement of cellular structure areas.

For widefield fluorescence microscopy, the cells were fixed and permeabilized in a solution of 0.05% Triton X-100 (Sigma, USA) in PBS for five minutes at 4°C. The cells were then washed with PBS and incubated with 3% BSA to block nonspecific binding.

DNA was stained with 1:1000 diluted Hoechst 33342 (Sigma, USA) in PBS and incubated for 30 minutes. Neutrophil membranes were visualized using a 1:500 dilution of Alexa Fluor 594-conjugated wheat germ agglutinin (WGA; Thermo Fisher Scientific, USA), and F-actin was stained with a 1:1000 dilution of Alexa Fluor 488-conjugated phalloidin (Thermo Fisher Scientific, USA). All staining steps were performed in the dark. After staining, the coverslips were washed three times with PBS, mounted onto microscope slides, and fixed using ibidi mounting medium (ibidi, Germany).

Statistical analysis was conducted using OriginPro 2019 (OriginLab Corporation, USA). Quantitative data were expressed as the median (*Me*) and interquartile range (*Q1; Q3*). The Shapiro–Wilk test was used to assess the distribution of variables. Since most parameters did not follow a normal distribution, nonparametric methods were employed. The Mann–Whitney *U* test was used to compare two independent groups and the Wilcoxon signed-rank test was used for paired data. The

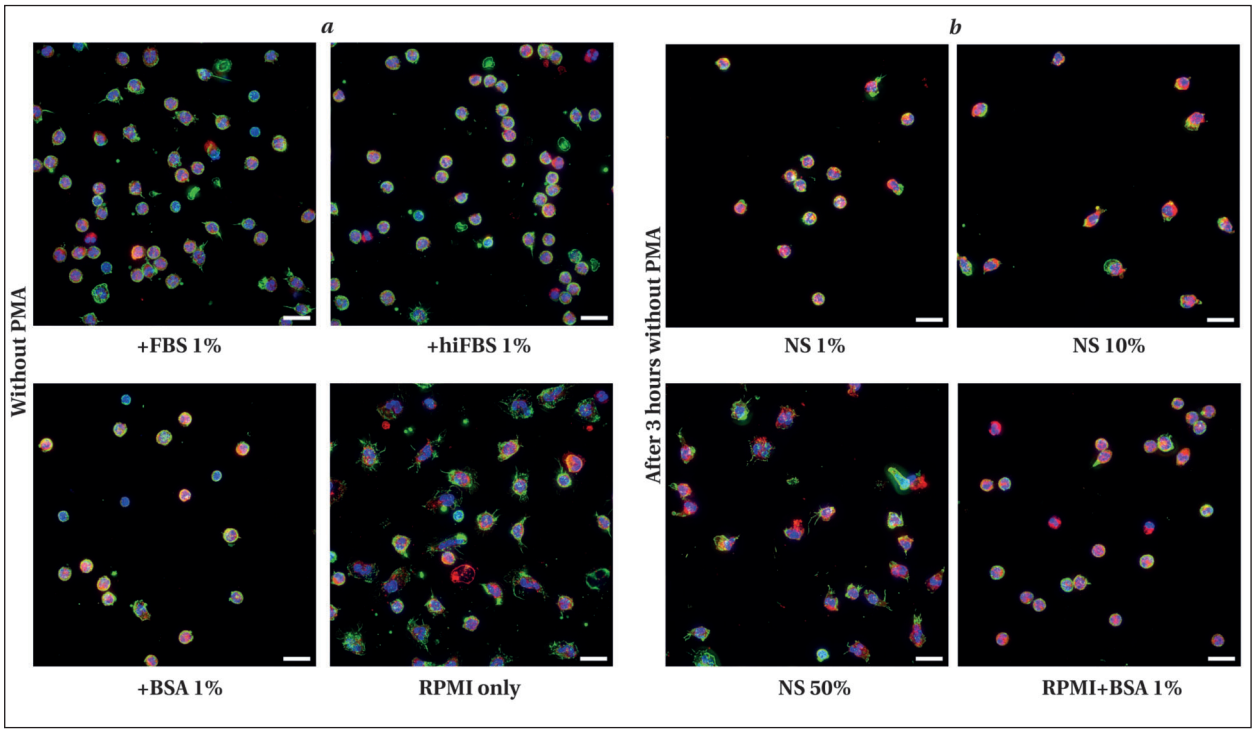


**Fig. 1. Fluorescence images of neutrophils under different incubation conditions: effect of medium components (*a*) and plasma concentration (*b*).**

**Note.** Blue indicates the nucleus, green indicates F-actin, and red indicates the membrane. Scale bar: 20 μm. FBS — fetal bovine serum; hiFBS — heat-inactivated fetal bovine serum; BSA — bovine serum albumin; NS — serum from apparently healthy (normal) newborns.

Kruskal–Wallis test was used to compare three independent groups, followed by a Dunn's multiple comparison test for post hoc analysis. Differences were considered statistically significant at $P<0.05$ (two-tailed).

## Results and Discussion

The initial phase of the study focused on optimizing the experimental conditions for the main investigation. The basal medium was RPMI supplemented with HEPES. The goal was to determine the appropriate additional components of the medium and the optimal concentrations of neonatal plasma and PMA.

As part of the preliminary experiments, we compared the effects of 1% fetal bovine serum (FBS), 1% heat-inactivated FBS (hiFBS), 1% bovine serum albumin (BSA), and the basal medium alone on neutrophil status. Neutrophil morphology was assessed under each condition. Incubation of neutrophils in the basal medium alone resulted in widespread adhesion to the glass surface, indicating premature cell activation. Adding 1% FBS, hiFBS, or BSA equally suppressed this premature activation (Fig. 1, *a*).

BSA at 1% produced the most suitable reduction in neutrophil adhesion under our experimental conditions.

To determine the optimal dose of neonatal plasma, we assessed the effect of varying plasma concentrations on neutrophils (Fig. 1, *b*). Specifically, we compared the effects of 1%, 10%, and 50% plasma supplementation versus the basal medium. Representative images of neutrophils are shown in Fig. 1, *b*.

Adding 1% plasma to the working medium best preserved neutrophils in their intact state, while 10% and 50% plasma concentrations promoted adhesion to the surface.

Neutrophils were activated using PMA. In studies on NETs, PMA is commonly applied at concentrations ranging from 1 to 100 nM. For this experiment, the optimal PMA concentration was defined as the minimal dose that induces neutrophil activation in the presence of plasma.

Representative images of control and PMA-activated neutrophils are presented in Fig. 2.

Fluorescence microscopy data were used to quantify the number of activated neutrophils that

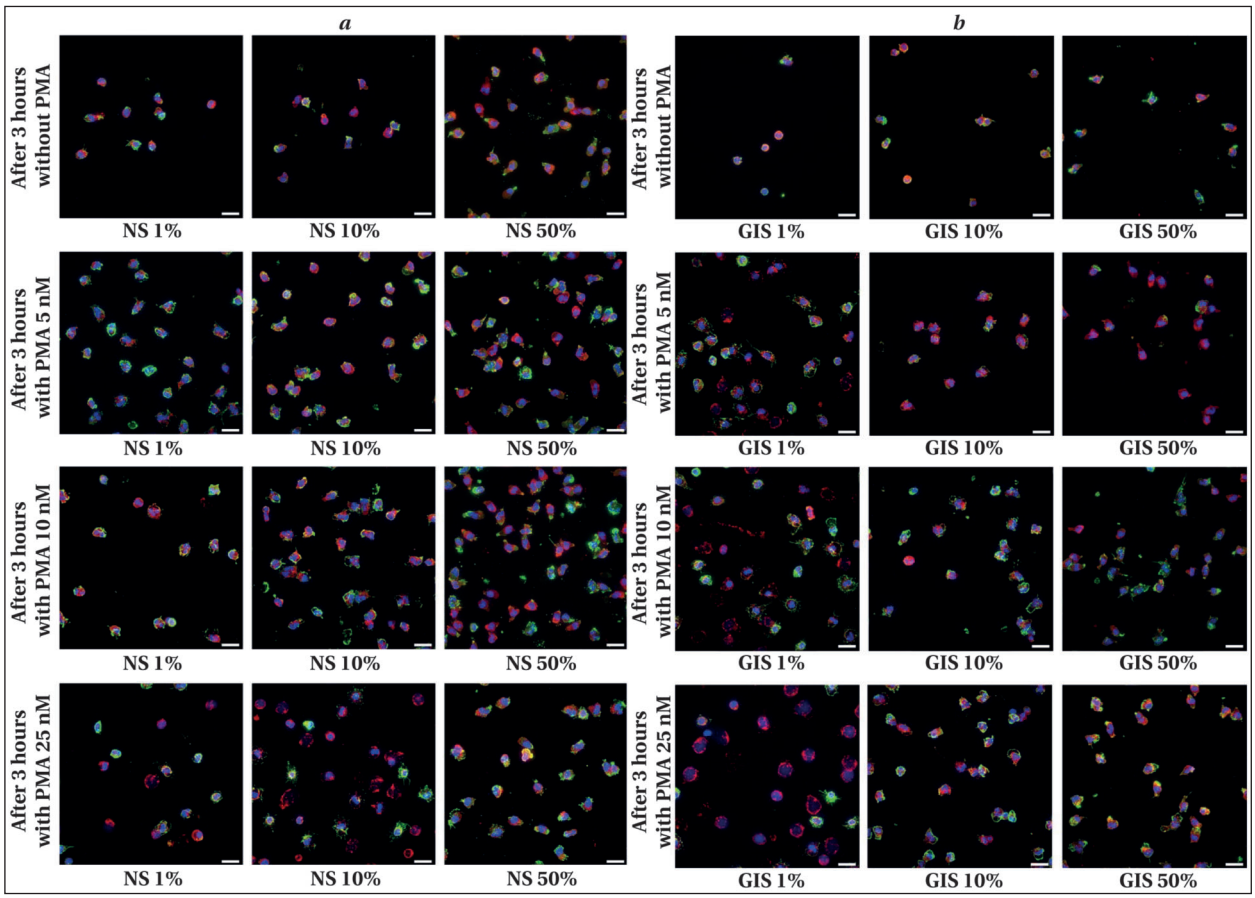


**Fig. 2. Fluorescence images of neutrophils in working medium with added plasma from an apparently healthy newborn, at varying PMA concentrations.**
**Note.** *a* — control neutrophils; *b* — neutrophils after activation. Blue indicates the nucleus, green indicates F-actin, and red indicates the membrane. Scale bar: 20 μm. NS — plasma samples from apparently healthy (normal) newborns; GIS — plasma samples from generalized infection group.

released NETs in each group. The analysis revealed that higher plasma concentrations, regardless of type, inhibited NET formation by neutrophils. The most effective condition for NET induction was observed with 1% plasma supplementation.

The number of NET-activated cells was calculated based on morphology and nuclear status. Representative fluorescence images used for quantification are shown in Fig. 3, *a* and 3, *b*.

Cells were considered NET-activated if they exhibited the following features: (1) disrupted segmented nuclear morphology, where the nucleus appeared as either a large «cloud» lacking structural organization or an elongated «arrow»-like shape; (2) absence of the actin cytoskeleton, where the presence of cortical actin is an indirect marker of functional integrity; and (3) the membrane no longer maintained a continuous structure. All other cells were classified as non-activated and intact. These included round or oval neutrophils with a diameter of 6–9 μm that exhibited segmented nuclei and cortical actin, as well as adherent cells with segmented nuclei that were spread across the glass surface and displayed prominent filopodia.

We analyzed morphological changes in neutrophils following incubation with various types of

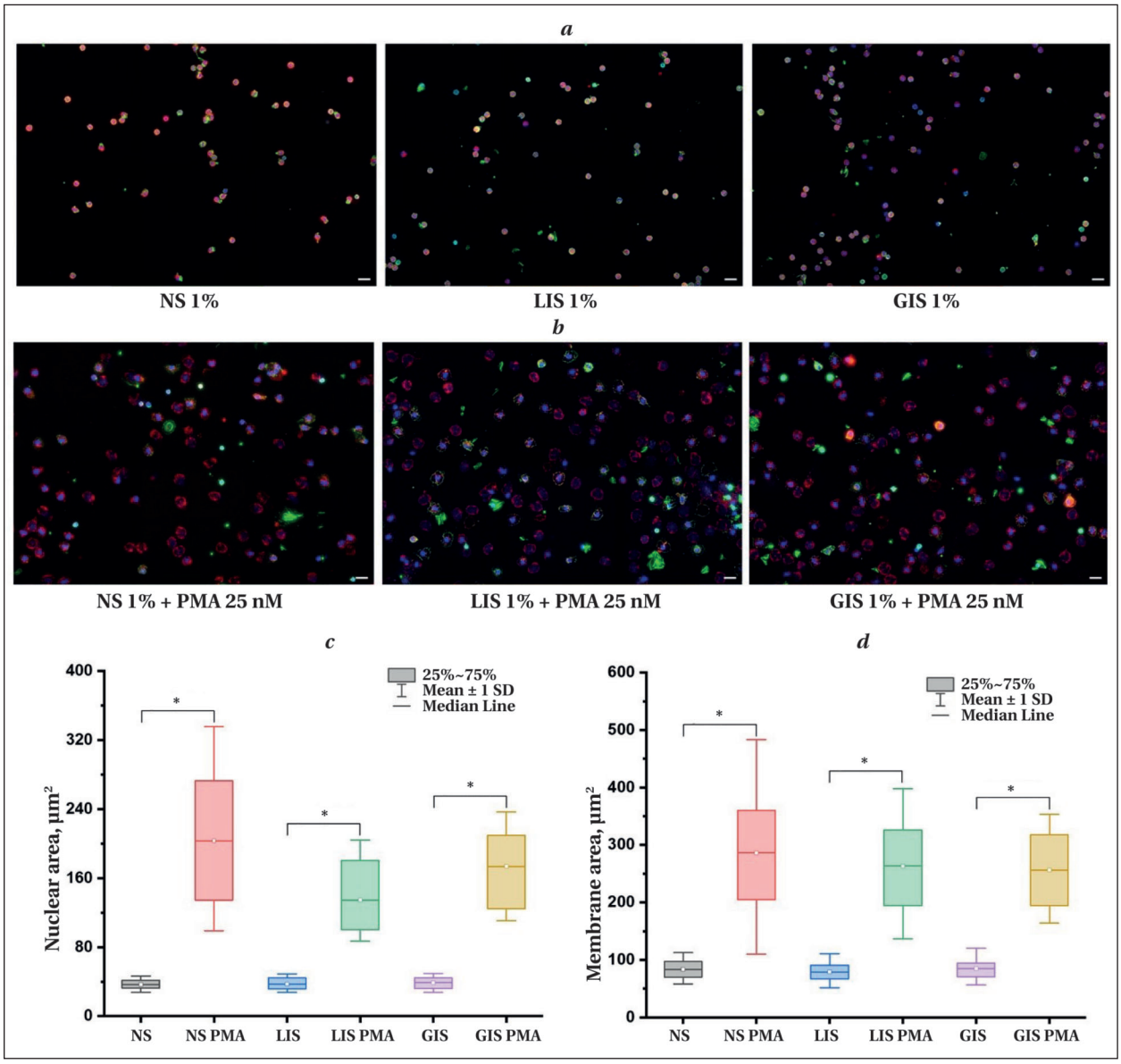


**Fig. 3. Effect of different plasma types on neutrophil morphological changes following PMA stimulation.**
**Note:** *a*, *b* — fluorescence images of neutrophils incubated with 1% plasma of various types, without stimulation (*a*) and after addition of PMA (*b*). Blue indicates the nucleus, green indicates F-actin, and red indicates the membrane. Scale bar: 20 μm. *c*, *d* — quantitative analysis of nuclear and membrane areas of neutrophils under different conditions. NS — serum from apparently healthy (normal) newborns; LIS — serum from newborns with localized infection; GIS — serum from newborns with generalized infection. Statistically significant differences within groups are indicated ($P<0.001$).

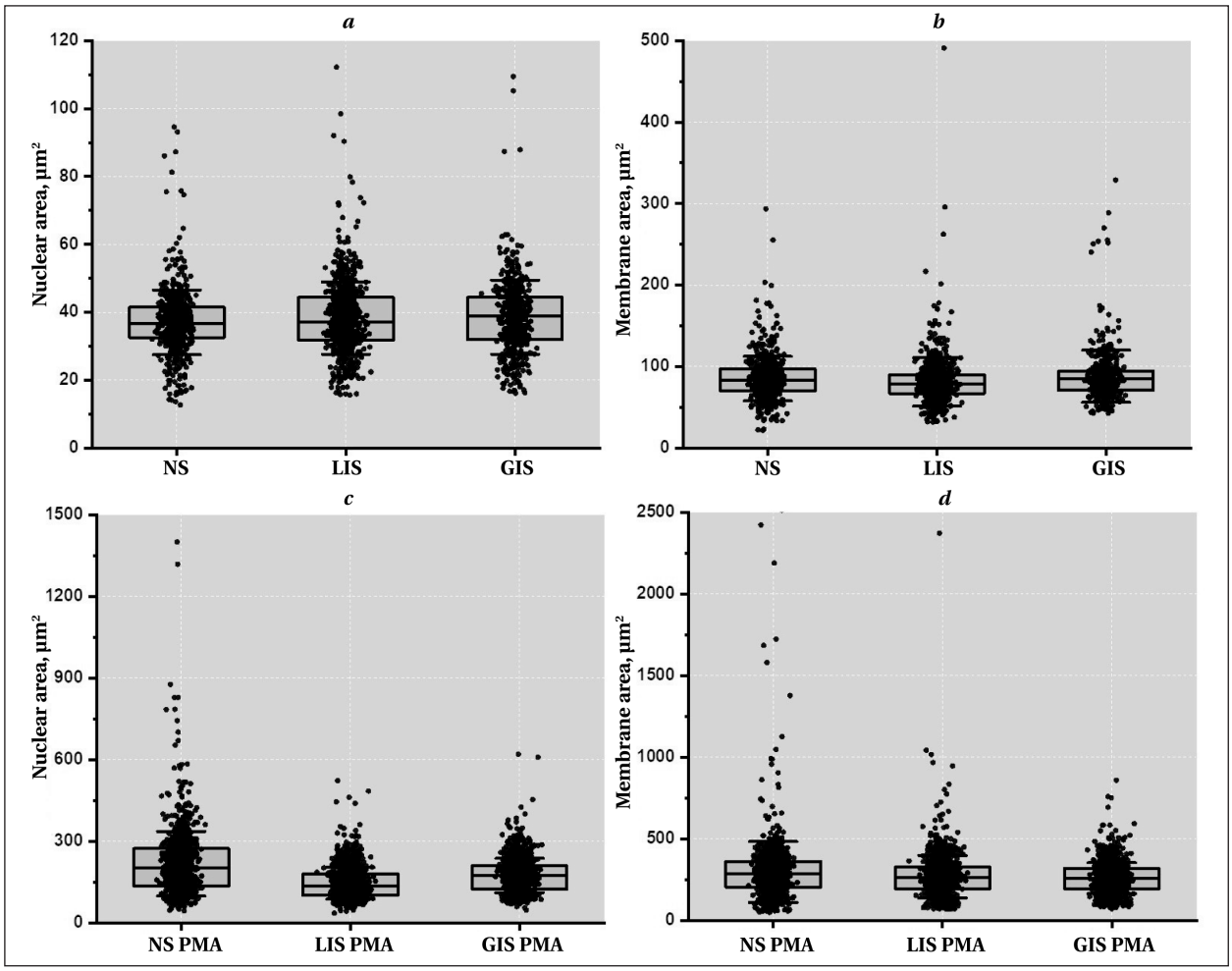


**Fig. 4. Graphs showing changes in neutrophil nuclear and membrane areas.**
**Note.** *a, b* — values prior to PMA stimulation; *c, d* — values after addition of PMA.

plasma and subsequent PMA stimulation. To this end, we examined the obtained fluorescent images and measured the areas of neutrophil nuclei and cytoplasmic membranes. It is well established that NET activation is accompanied by nuclear swelling and an increase in overall cell size [26] (Fig. 3, *c*, *d*). Following PMA stimulation, we observed a significant increase in nuclear area: in the NS group, from 37 μm² (33–42 μm²) to 203 μm² (135–273 μm²) ($P$<0.001); in the LIS group, from 37 μm² (32–44 μm²) to 134 μm² (101–180 μm²) ($P$<0.001); and in the GIS group, from 39 μm² (32–44 μm²) to 173 μm² (124–210 μm²) ($P$<0.001). Similar trends were observed for membrane area: NS, from 83 (70; 97) to 286 (205; 361) μm² ($P$<0.001); LIS, from 79 (67; 90) to 263 (194; 326) μm² ($P$<0.001); and GIS, from 85 (70; 95) to 256 (195; 318) μm² ($P$<0.001).

Analysis of the graphs revealed that non-activated neutrophils retained their segmented nuclear morphology and spherical shape. Following PMA stimulation, neutrophils exhibited a significant increase in nuclear and membrane area. At the same time, there was considerable variation in morphological parameters within the same plasma group, indicating heterogeneity in the effect of plasma on cells. Despite this variability, the general trend of morphological changes associated with NET activation was observed across all examined samples.

Figure 4 presents distribution plots of all measured nuclear and membrane areas of neutrophils before and after PMA stimulation, stratified by plasma type. Neutrophils incubated with plasma from neonates with generalized infection exhibited a significantly larger nuclear area prior to PMA stimulation compared to those treated with control plasma ($\chi^2$=9.366; $P$=0.009).

After PMA activation, the distribution pattern of nuclear area values changed. The largest nuclear area was recorded in neutrophils incubated with plasma from apparently healthy neonates. Next were those exposed to plasma from the GIS group, followed by those treated with plasma from patients with localized infection ($\chi^2$=339.295; $P$<0.001).

A similar trend was observed for the membrane area. Before PMA activation, the smallest membrane areas were found in neutrophils incubated with plasma from the LIS group ($\chi^2$ = 26.396; $P$<0.001). However, after PMA stimulation, the largest mem-

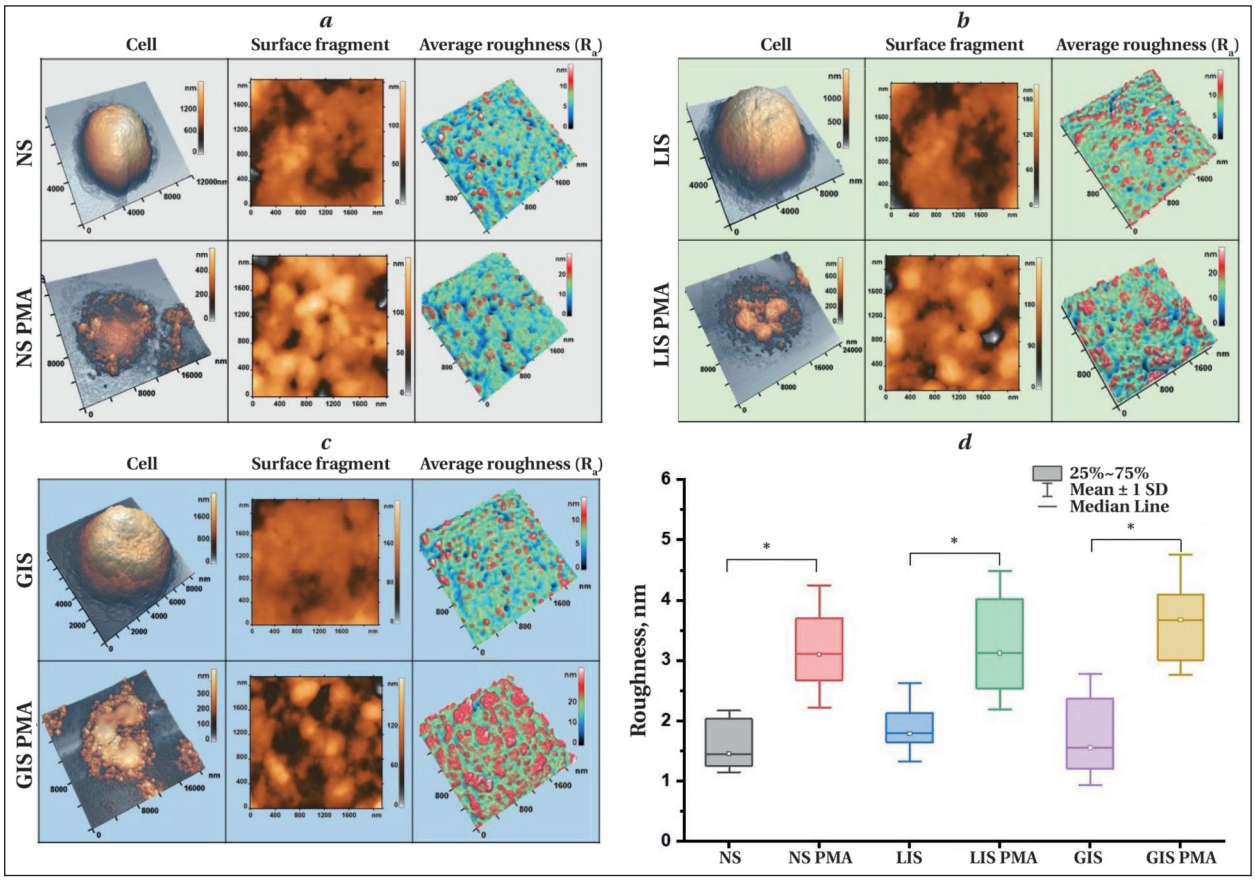


**Fig. 5. AFM images of neutrophils and analysis of membrane roughness after exposure to plasma from different groups.**
**Note.** *a–c* — 3D images of neutrophils (first column), membrane surface fragments (second column), and corresponding $R_a$ maps (third column), obtained by atomic force microscopy (AFM) after incubation with plasma from the control group (NS) and from patients with localized (LIS) or generalized (GIS) infection, before and after PMA stimulation. *d* — graph showing changes in average membrane surface roughness across all experimental groups. Statistically significant within-group differences are indicated ($P<0.001$).

brane areas were found in neutrophils treated with control plasma ($\chi^2=37.663$; $P<0.001$).

Fig. 5 shows the mean membrane roughness values of neutrophils measured by AFM. Comparing non-activated groups, neutrophils incubated with plasma from apparently healthy donors, as well as those from LIS and GIS patients, demonstrated comparable roughness values. $R_a$ values were 1.4 (1.2; 2.0) nm for NS, 1.8 (1.6; 2.1) nm for LIS, and 1.5 (1.2; 2.4) nm for GIS. Differences between groups were not statistically significant ($\chi^2=4.001$; $P=0.135$).

Detailed topographic images of neutrophil surfaces obtained by AFM were used for further analysis of cell surface features (Fig. 5, *a–c*).

After PMA activation, the membrane's shape changed significantly. All the studied groups had significantly higher $R_a$ values than their non-activated controls. Neutrophils exposed to plasma from the NS group in the presence of PMA increased in $R_a$ to 3.1 (2.7; 3.7) nm. The $R_a$ values were 3.1 (2.5; 4.0) and 3.7 (3.0; 4.0) nm in the LIS and GIS PMA groups, respectively. While there was a general trend towards higher roughness, an intergroup comparison revealed a *P*-value of 0.072 ($\chi^2=5.255$), indicating no significant differences across groups. However, pairwise comparisons of PMA-activated and non-activated groups showed significant differences ($P<0.001$), indicating that activation affects membrane roughness characteristics.

The increase in $R_a$ reflects the increased heterogeneity of the neutrophil surface after activation. Furthermore, PMA stimulation caused significant lateral expansion of the cells, consistent with recognized morphological characteristics of NET activation.

Fluorescence microscopy results showed that none of the plasma samples examined, regardless of patient group, had a deleterious effect on neutrophil morphology. The vast majority of cells in the control group, which did not receive PMA stimulation, maintained their morphology.

Neutrophils incubated with plasma from patients with localized infections exhibited the weakest response to stimulation, as indicated by nuclear area measurements. In contrast, neutrophils exposed to plasma from patients with generalized infections demonstrated comparable levels of NET activation to those in the control group. These results imply that the soluble factor profile in plasma from

localized infections stabilizes neutrophils within the circulation. Conversely, neutrophils appear more susceptible to chromatin network formation in the context of systemic infection, which may increase the risk of thrombosis and disseminated intravascular coagulation (DIC) in septic patients [30].

The results of the AFM analysis confirmed that, regardless of its origin, plasma did not have a significant damaging effect on neutrophils. In the absence of stimulation, neutrophils incubated with different plasma types maintained comparable membrane roughness values, indicating no substantial structural alterations. Upon PMA stimulation, all groups exhibited a similar increase in Ra values, reflecting a consistent rise in membrane surface heterogeneity. These observations suggest that NET-associated morphological changes to the cell surface occur to a similar extent, regardless of plasma origin.

**Limitations.** This study is limited by its relatively small sample size and the absence of neutrophil phenotypic characterization following incubation with plasma from neonates with varying degrees of infectious and septic complications.

## Conclusion

Our findings shed light on the mechanisms underlying neutrophil alterations in neonates during infectious and septic conditions. These findings may also aid in developing new diagnostic and therapeutic approaches. We showed that plasma has different effects on neutrophil NET activation depending on the severity of the infectious and septic condition.

Based on these findings, future research could employ advanced biochemical and biophysical assays, along with flow cytometry, to examine the molecular composition of plasma and its influence on neutrophil responses. These approaches could help us better understand the signaling pathways and effector mechanisms that control neutrophil activation.

The methodology used here and its refinement pave the way for more in-depth investigations into the pathophysiology of neonatal sepsis. Changes in neutrophil membrane properties induced by plasma may be useful biomarkers for determining the severity of infectious and septic conditions in newborns.

**Acknowledgments.** The authors gratefully acknowledge the staff of the Core Facility Center at the N. K. Koltsov Institute of Developmental Biology of the Russian Academy of Sciences. Special thanks are extended to Dr. Elena E. Voronezhskaya, Head of the Center, for her invaluable support with fluorescence microscopy.

## References


1. *Liu D., Huang S. Y., Sun J. H., Zhang H. C., Cai Q. L., Gao C., Li L., et al.* Sepsis-induced immunosuppression: mechanisms, diagnosis and current treatment options. *Mil Med Res.* 2022; 9 (1): 56. DOI: 10.1186/s40779-022-00422-y. PMID: 36209190.
2. *Понасенко А. В., Синицкий М. Ю., Хуторная М. В., Барбараш О. Л.* Генетические макеры системной воспалительной реакции в кардиохирургии (обзор). *Общая реаниматология.* 2017; 13 (6): 48–59. *Ponasenko A. V., Sinitsky M. Y., Khutornaya M. V., Barabash O. L.* Genetic markers of systemic inflammatory response in cardiac surgery (Review). *Gen Reanimatol = Obshchaya Reanimatologiya.* 2017; 13 (6): 48–59. (in Russ.&Eng.). DOI: 10.15360/1813-9779-2017-6-48-59.
3. *Mellhammar L., Wollter E., Dahlberg J., Donovan B., Olséen C.-J., Wiking P. O., Rose N., et al.* Estimating sepsis incidence using administrative data and clinical medical record review. *JAMA Netw Open.* 2023; 6 (8): e2331168. DOI: 10.1001/jamanetworkopen.2023.31168. PMID: 37642964.
4. *Образцов И. В., Рябов А. Ю., Цуранова Н. С., Балыкова Е. В., Парамонов А. И.* Функциональная активность нейтрофилов у пациентов с послеоперационными инфекционно-септическими осложнениями. *Российский иммунологический журнал.* 2019; 22 (4): 1393–401. *Obraztsov I. V., Ryabov A.Yu., Tsuranova N. S., Balykova E. V., Paramonov A. I.* Neutrophil function in patients with postsugery infectious septic complications. *Russian Journal of Immunology = Ross Immunol Zhurnal.* 2019; 22 (4): 1393–1401. (in Russ.). DOI: 10.31857/S102872210007042-1.
5. *Celik I. H., Hanna M., Canpolat F. E., Mohan Pammi.* Diagnosis of neonatal sepsis: the past, present and future. *Pediatr Res.* 2022; 91 (2): 337–350. DOI: 10.1038/s41390-021-01696-z. PMID: 34728808.
6. *Glaser M. A., Hughes L. M., Jnah A., Newberry D.* Neonatal sepsis: a review of pathophysiology and current management strategies. *Adv Neonatal Care.* 2021; 21 (1): 49–60. DOI: 10.1097/ANC.0000000000000769. PMID: 32956076.
7. *Образцов И. В., Жиркова Ю. В., Черникова Е. В., Крапивкин А. И., Брунова О. Ю., Абдраисова А. Т., Давыдова Н. В.* Значение функционального анализа фагоцитов для диагностики неонатального сепсиса. *Российский вестник перинатологии и педиатрии.* 2023; 68 (1): 24–29. *Obraztsov I. V., Zhirkova Y. V., Chernikova E. V., Krapivkin A. I., Brunova O. Y., Abdraisova A. T., Davydova N. V.* Feasibility of phagocytes functional testing in neonatal sepsis diagnostics. *Russian Bulletin of Perinatology and Pediatrics = Rossiyskiy Vestnik Perinatologii i Pediatrii.* 2023; 68 (1): 24–29. (in Russ.). DOI: 10.21508/1027-4065-2023-68-1-24-29.
8. *Ohbuchi A., Kono M., Kitagawa K., Takenokuchi M., Imoto S., Saigo K.* Quantitative analysis of hemin-induced neutrophil extracellular trap formation and effects of hydrogen peroxide on this phenomenon. *Biochem Biophys Reports.* 2017; 11: 147–153. DOI: 10.1016/j.bbrep.2017.07.009. PMID: 28955779.
9. *Parker H., Winterbourn C. C.* Reactive oxidants and myeloperoxidase and their involvement in neutrophil extracellular traps. *Front Immunol.* 2012; 3: 424. DOI: 10.3389/fimmu.2012.00424. PMID: 23346086.
10. *Zhang J., Shao Y., Wu J., Zhang J., Xiong X., Mao J.,Wei Y., et al.* Dysregulation of neutrophil in sepsis: recent insights and advances. *Cell Commun Signal.* 2025; 23 (1): 87. DOI: 10.1186/s12964-025-02098-y. PMID: 39953528.
11. *Sergunova V., Inozemtsev V., Vorobjeva N., Kozlova E., Sherstyukova E., Lyapunova S., Chernysh A.* Morphology of neutrophils during their activation and NETosis: atomic force microscopy study. *Cells.* 2023; 12 (17): 2199. DOI: 10.3390/cells12172199. PMID: 37681931.
12. *Dewitt S., Hallett M.* Leukocyte membrane «expansion»: a central mechanism for leukocyte extravasation. *J Leukoc Biol.* 2007; 81 (5): 1160–4. DOI: 10.1189/jlb.1106710. PMID: 17360954.
13. *Hallett M. B., Dewitt S.* Ironing out the wrinkles of neutrophil phagocytosis. *Trends Cell Biol.* 2007; 17 (5): 209–14. DOI: 10.1016/j.tcb.2007.03.002. PMID: 17350842.
14. *Гребенчиков О. А., Касаткина И. С., Каданцева К. К., Мешков М.А., Баева А. А.* Влияние лития хлорида на активацию нейтрофилов под действием сыворотки пациентов с септическим шоком. *Общая реаниматология.* 2020; 16 (5): 45–55. *Grebenchikov O. A., Kasatkina I. S., Kadantseva K. K., Meshkov M. A., Bayeva A. A.* The effect of lithium chloride on neutrophil activation on exposure to serum of patients with septic shock. *Gen Reanimatol = Obshchaya Reanimatologiya.* 2020; 16 (5): 45–55. (in Russ.&Eng.). DOI: 10.15360/1813-9779-2020-5-45-55.
15. *Образцов И. В., Годков М. А., Кулабухов В. В., Владимирова Г. А., Измайлов Д. Ю., Проскурнина Е. В.* Функциональная активность нейтрофилов при ожоговом сепсисе. *Общая реаниматология.* 2017; 13 (2): 40–51. *Obraztsov I. V., Godkov M. A., Kulabukhov V. V., Vladimirova G. A., Izmailov D. Y., Proskurnina E. V.* Functional activity of neutrophils in burn sepsis. *Gen Reanimatol = Obshchaya Reanimatologiya.* 2017; 13 (2): 40–51. (in Russ.&Eng.). DOI: 10.15360/1813-9779-2017-2-40-51.
16. *Starostin D. O., Kuzovlev A. N., Dolgikh V. T., Grebenchikov O. A., Polyakov P. A., Grechko A. V.* Influence of sevoflurane on neutrophils in patients with sepsis. *Russ J Anesthesiol Reanimatol.* (in Russ.&Eng.). 2024; (5): 50. DOI: 10.17116/anaesthesiology202405150.
17. *Liu S., Han Y., Kong L., Wang G., Ye Z.* Atomic force microscopy in disease-related studies: exploring tissue and cell mechanics. *Microsc Res Tech.* 2024; 87 (4): 660–684. DOI: 10.1002/jemt.24471. PMID: 38063315.
18. *Dumitru A. C., Koehler M.* Recent advances in the application of atomic force microscopy to structural biology. *J Struct Biol.* 2023; 215 (2): 107963. DOI: 10.1016/j.jsb.2023.107963. PMID: 37044358.
19. *Kerdegari S., Canepa P., Odino D., Oropesa-Nuñez R., Relini A., Cavalleri O., Canale C.* Insights in cell biomechanics through atomic force microscopy. *Mate-*

*rials (Basel)*. 2023; 16 (8): 2980.
DOI: 10.3390/ma16082980. PMID: 37109816.
20. *Sokolov I., Iyer S., Woodworth C. D.* Recovery of elasticity of aged human epithelial cells *in vitro*. *Nanomedicine*. 2006; 2 (1): 31–36.
DOI: 10.1016/j.nano.2005.12.002. PMID: 17292113.
21. *Pérez-Domínguez S., Kulkarni S. G., Rianna C., Radmacher M.* Atomic force microscopy for cell mechanics and diseases. *Neuroforum*. 2020; 26 (2): 101–109. DOI: 10.1515/nf-2020-0001.
22. *Makarova N., Kalaparthi V., Seluanov A., Gorbunova V., Dokukin M. E., Sokolov I.* Correlation of cell mechanics with the resistance to malignant transformation in naked mole rat fibroblasts. *Nanoscale*. 2022; 14 (39): 14594–14602.
DOI: 10.1039/D2NR01633h. PMID: 36155714.
23. *Burn G. L., Foti A., Marsman G., Patel D. F., Zychlinsky A.* The Neutrophil. *Immunity*. 2021; 54 (7): 1377–1391.
DOI: 10.1016/j.immuni.2021.06.006. PMID: 34260886.
24. *Tilley D. O., Abuabed U., Arndt U. Z., Schmid M., Florian S., Jungblut P. R., Brinkmann V., et al.* Histone H3 clipping is a novel signature of human neutrophil extracellular traps. *Elife*. 2022; 11: e68283.
DOI: 10.7554/eLife.68283. PMID: 36282064.
25. *Thiam H. R., Wong S. L., Qiu R., Kittisopikul M., Vahabikashi A., Goldman A. E., Goldman R. D., et al.* NETosis proceeds by cytoskeleton and endomembrane disassembly and PAD4-mediated chromatin decondensation and nuclear envelope rupture. *Proc Natl Acad Sci*. 2020; 117 (13): 7326–7337.
DOI: 10.1073/pnas.1909546117. PMID: 32170015.
26. *Inozemtsev V., Sergunova V., Vorobjeva N., Kozlova E., Sherstyukova E., Lyapunova S., Chernysh A.* Stages of NETosis Development upon Stimulation of Neutrophils with Activators of Different Types. *Int J Mol Sci*. 2023; 24 (15): 12355.
DOI: 10.3390/ijms241512355. PMID: 37569729.
27. *Wei M., Zhang Y., Wang Y., Liu X., Li X., Zheng X.* Employing atomic force nicroscopy (AFM) for microscale investigation of interfaces and interactions in membrane fouling processes: new perspectives and prospects. *Membranes (Basel)*. 2024; 14 (2): 35.
DOI: 10.3390/membranes14020035. PMID: 38392662.
28. *Миронов В. Л.* Основы сканирующей зондовой микроскопии. Нижний Новгород: Российская академия наук, Институт физики микроструктур; 2004: 110. *Mironov V. L.* Fundamentals of scanning probe microscopy. Nizhny Novgorod: Russian Academy of Sciences, Institute of Physics of Microstructures; 2004: 110. (in Russ.).
29. *Schneider C. A., Rasband W. S., Eliceiri K. W.* NIH Image to imageJ: 25 years of image analysis. *Nat Methods*. 2012; 9 (7): 671–675.
DOI: 10.1038/nmeth.2089. PMID: 22930834.
30. *Zhou Y., Xu Z., Liu Z.* Impact of neutrophil extracellular traps on thrombosis formation: new findings and future perspective. *Front Cell Infect Microbiol*. 2022; 12: 910908.
DOI: 10.3389/fcimb.2022.910908. PMID: 35711663.

**Received 01.04.2025**
**Accepted 27.05.2025**
**Online first 09.06.2026**